Article ID: 1003－6326(2005)04－0851－04

ZrB_2/Al_2O_3 composite powders prepared by self-propagating high-temperature synthesis①

YU Zhi-qiang(于志强), YANG Zhen-guo(杨振国)
(Department of Material Science, Fudan University, Shanghai 200433, China)

Abstract: Self-propagating high-temperature synthesis(SHS) method was used to synthesize ZrB_2/Al_2O_3 composite powders from B_2O_3-ZrO_2-Al system. X-ray diffractometry(XRD) and scanning electron microscopy(SEM) analyses show the presence of ZrB_2 and Al_2O_3 as the primary phases in the composite powders, while the presence of a very small amount of ZrO_2 is thought to be unreacted zirconium oxide. Transmission electron microscopy(TEM) and high resolution electron microscopy(HREM) observations of microstructure of the composite powders indicate that the interfaces of ZrB_2/Al_2O_3 bond well without any interfacial reaction products. It is proposed that the good interfacial bonding of composite powders results from the ZrB_2 particles crystallizing and growing on the Al_2O_3 particles surface with surface defects acting as nucleation centers.

Key words: self-propagating high-temperature synthesis; zirconium diboride; composite powder; $B_2O_3+ZrO_2+$Al system; microstructure

CLC number: TB332 **Document code:** A

1 INTRODUCTION

The borides and/or boron compounds, e.g. ZrB_2 and TiB_2, have excellent physical and chemical properties such as high melting point, high hardness, high electrical conductivity, good corrosion resistance against molten iron and slags and superb thermal shock resistance. Such unique properties make them attractive candidates for a range of applications as cutting tool, light mass protective armor, wear-resistant materials, corrosion and absorption-resistant materials and cathode materials for aluminum refinement furnace[1-4]. Despite the excellent properties, their applicability is restricted. This is undoubtedly related to the costs associated with production of the raw powders and the fabrication of the monolithic and composite components. Conventionally, these materials are processed by arc melting, varpour deposition and plasma synthesis[5]. But the production costs are elevated because of high energy requirement and the complexity of equipment. Self-propagating high temperature synthesis(SHS) has been shown to be an effective way to produce these materials such as TiB_2, ZrB_2, CaB_6, TiB_2-Al_2O_3 and TiB_2-TiC[6-10]. The SHS technique has inherent advantages over the other methods that require high-temperature furnaces and longer processing time. Materials produced by the SHS method have some obvious advantages which include higher purity of the products, low energy requirements, relative simplicity of the process, and low cost[11-13]. In addition, due to the high cooling rates and high defect concentrations, nonequilibrium metastable structures are expected to exist in the SHS-produced powders, resulting in more reactive and enhanced sinterability of the powders[14, 15].

Recently, some reports on study of the borides and composites prepared by SHS have generally concentrated on titanium diboride and composites[6-8], and zirconium diboride ceramics, but ceramic powder composites containing zircorium diboride has not been sufficiently studied. In the present work, zirconium diboride-alumina composite powders are prepared by SHS with cheap raw materials, such as oxides of zirconium and boron. The phase compositions of composite powders are analyzed and the microstructures are also characterized.

2 EXPERIMENTAL

Amorphous boron oxide powder(mean particle size below 44 μm, purity 99.8%), zirconium oxide powder(mean particle size below 50 μm, purity 99.1%) and reducing agent aluminum powder (mean particle size below 50 μm, purity 99.9%) were used as reactants for the synthesis. The mixture was prepared as stoichiometry of reaction (1):

$$3ZrO_2+3B_2O_3+10Al \rightarrow 3ZrB_2+5Al_2O_3 \quad (1)$$

The mixtures were homogenized by dry ball milling, then the mixtures were cold pressed into cylinder pellets with diameter of 40 mm and height

① **Foundation item:** Project(KNH2021005) supported by Industrialization Program of Economic Committee of Shanghai
Received date: 2004－12－08; **Accepted date:** 2005－03－08
Correspondence: YANG Zhen-guo, Professor; Tel: +86-21-65642523; E-mail: zgyang@fudan.edu.cn; yuzhiqiang252@sohu.com

of 60 mm. The pressure used was sufficient to give a green relative density of about 55%. SHS of ZrB_2/Al_2O_3 was carried out in a stainless steel reactor under a protective atmosphere of Ar. The reactant pellets were ignited at one corner by a high-energy heat input. A W-3%Re/W-25%Re thermocouple inserted along the cylinder axis in the bottom of the sample was used to measure the temperature during the synthesis process. The ignition source was switched off as the surface reached the required ignition temperature and the combustion wave propagated throughout the sample. After the reaction, the synthesized products were treated by ball-milling to produce fine powder. The crystalline phases were characterized with a Philips X-ray Diffractometer(XRD, Holland). The microstructure and composition analysis were carried out using a scanning electron microscope (SEM) (JEOL-JSM 800, Japan), a JEOL-200CX transmission electron microscope(TEM) with an accelerating voltage of 200 kV and energy dispersive X-ray(EDX) (KEVEX, USA), respectively. The interface of composite powders was analyzed using a JEOL-2010CF high resolution transmission electron microscope(HREM) operated at 200 kV.

3 RESULTS AND DISCUSSION

3.1 Powders examination

Fig. 1 shows the XRD pattern of the synthesized powders. The pattern reveals the expected zirconium diboride as well as alumina peaks corresponding to the α-Al_2O_3 polymorph. In the low angle region, a ZrO_2 peak is identified. This indicates that the composite powders are made up of ZrB_2, α-Al_2O_3 and ZrO_2. By comparing relative intensity values determined from the strongest diffraction peak of each phase, the relative amount of ZrB_2 and Al_2O_3 phases is much larger than that of ZrO_2.

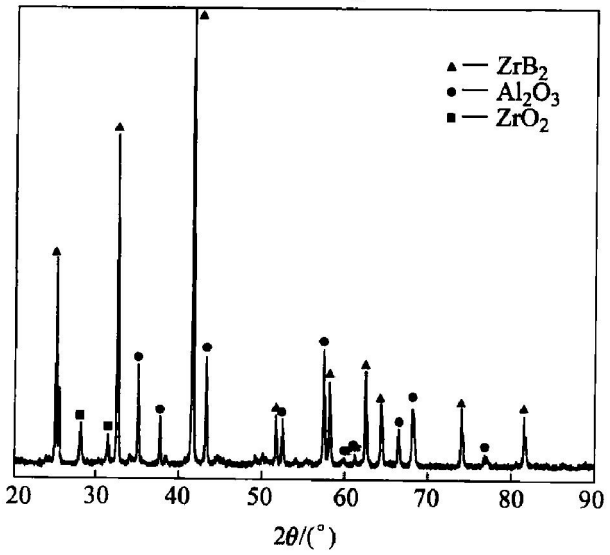

Fig. 1 XRD pattern of synthesized powders

This shows the presence of ZrB_2 and Al_2O_3 as the primary phase in the powders. The presence of a very small amount of ZrO_2 is thought to be unreacted zirconium oxide.

Fig. 2 shows the SEM image of the composite powders synthesized by SHS. The prepared powders are clearly of micrometer size. Chemical composition analysis of the powders shows the presence of Zr, B, Al and O. It can be deduced that ZrB_2 and Al_2O_3 appear in the synthesized samples.

Figs. 3(a) and 3(b) show the particle size distribution curves of ZrB_2 monolithic particles and ZrB_2-Al_2O_3 composite particles synthesized by SHS, respectively. By comparing Fig. 3(a) with Fig. 3(b), the monolithic particles(a) are charac-

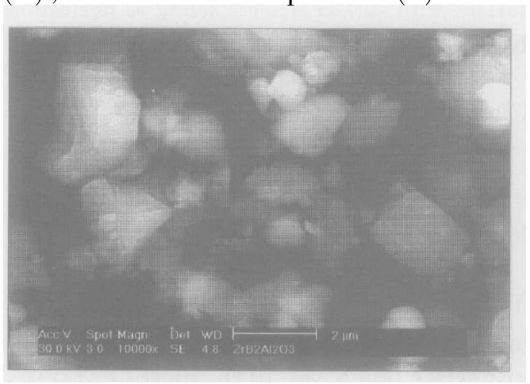

Fig. 2 SEM image of composite powders

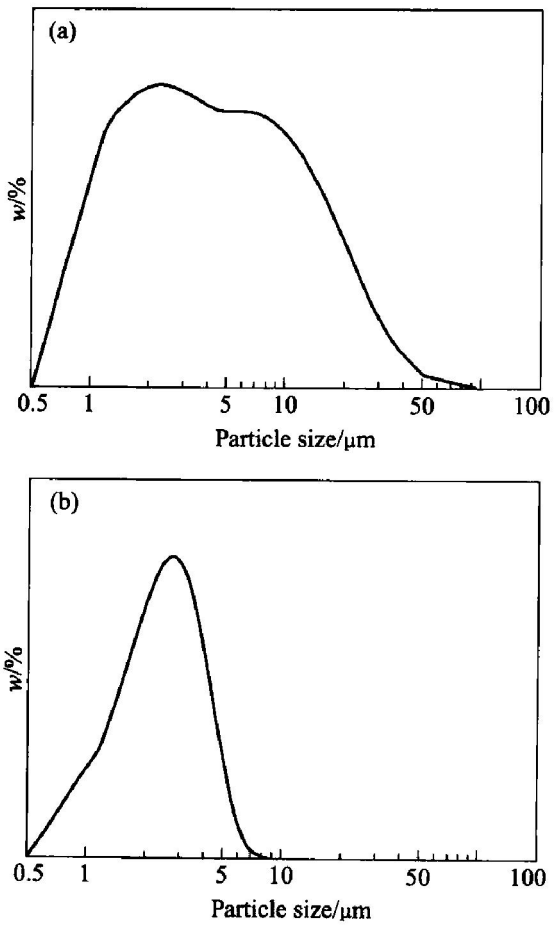

Fig. 3 Particle size distributions of powders
(a) —ZrB_2 monolithic particles;
(b) —ZrB_2-Al_2O_3 composite particles

terized by a comparatively wide size distribution. Their mean particle size is bigger(> 5 μm). While the composite particle (b) size distribution is obviously narrow, and the mean particle size decreases (2 - 4 μm). This is mainly related to the good interface formation among the different particles in composite powders during the synthesis reaction. This interfaces can inhibit the grain growth of the particles and finally lead to decrease in the particle macroscopic size.

3.2 Microstructure characterization

The TEM image of composite particles is shown in Fig. 4. It can be seen that the single particle is of sub-micron size, and particles joint each other. Fig. 4(b) shows the interface among particle compounds well.

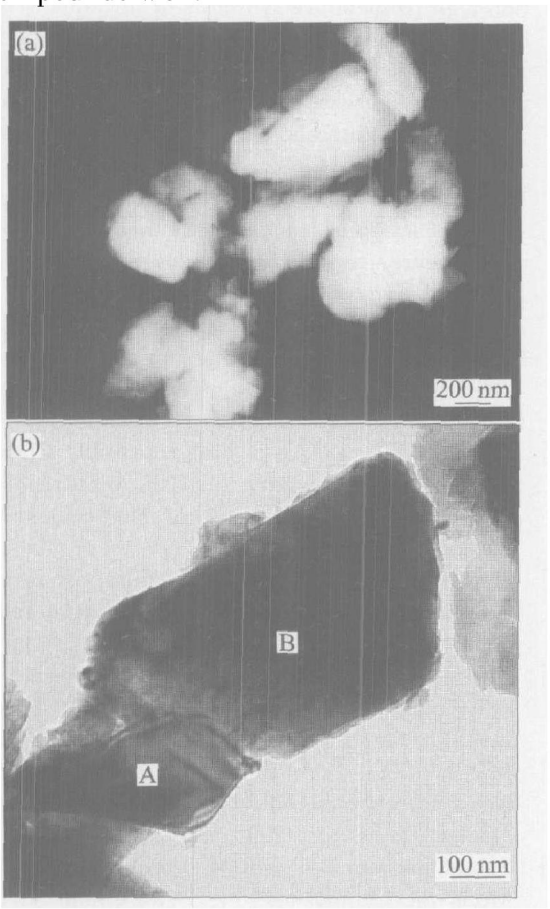

Fig. 4 TEM images of composite particles
(a) —Low magnification; (b) —High magnification

In order to define the chemical compositions, the EDS analysis of composite particles was conducted. Fig. 5(a) and Fig. 5(b) show the EDS patterns of particles A and B(in Fig. 4(b)), respectively. As seen from Fig. 5, particle A is a phase with high zirconium and boron contents, while particle B with high aluminum and oxide contents. As analyzed above, it can be defined that A is ZrB_2 particle and B is Al_2O_3 particle. This indicates that the ZrB_2 and Al_2O_3 particles joint well in composite powders prepared by SHS.

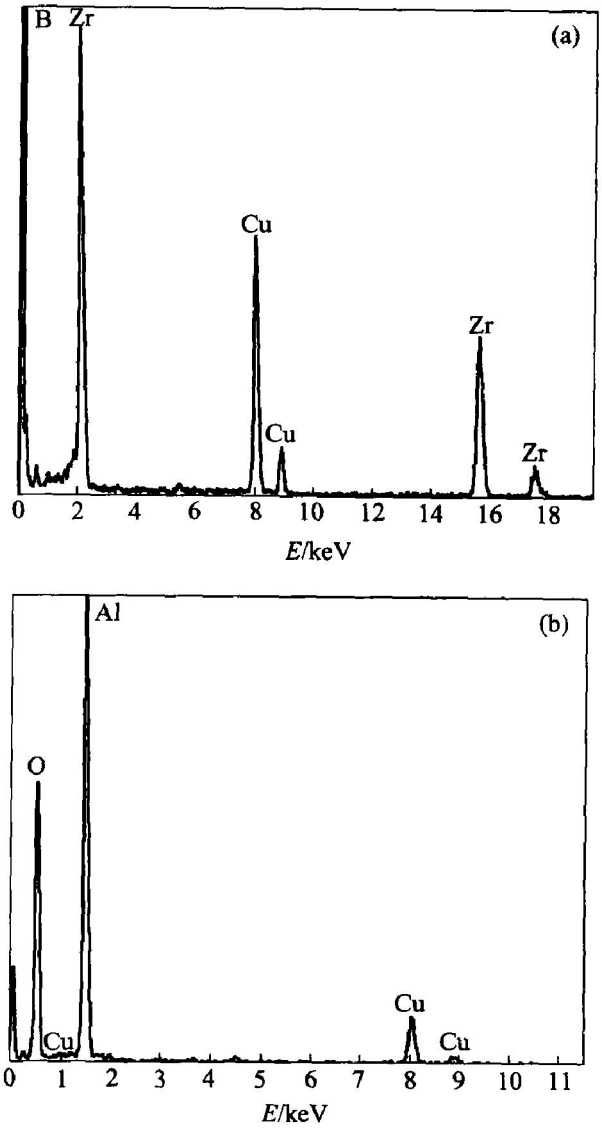

Fig. 5 EDS analysis results of composite particles
(a) —Particle A; (b) —Particle B

In order to further analyze the interfacial bonding state between ZrB_2 and Al_2O_3 particles, HREM observations of interfaces were performed. Fig. 6 shows the interfacial HREM images of Fig. 4 (b) along the [441] orientation of the Al_2O_3 particle and the $[01\bar{1}1]$ orientation of the ZrB_2 particle, respectively.

Fig. 6 shows that the interfaces bond directly, free from interfacial reactants and precipitates. It can be found that the interface compounds well though no regular lattice array resulting from two phases interweaving each other can be observed in the interfaces.

The formation of this interfacial structure can be suggested to be related to the crystallization process of ZrB_2 particles. According to analysis, in B_2O_3-ZrO_2-Al chemical system, B_2O_3 is first melted. Because of the diffusion between solid phase (Al) and liquid phase(B_2O_3), the following reductive reactions can be initiated:

$$B_2O_3(l) + 2Al(s) \rightarrow 2B(s) + Al_2O_3(s) \quad (2)$$

After melting of Al powder, the following two

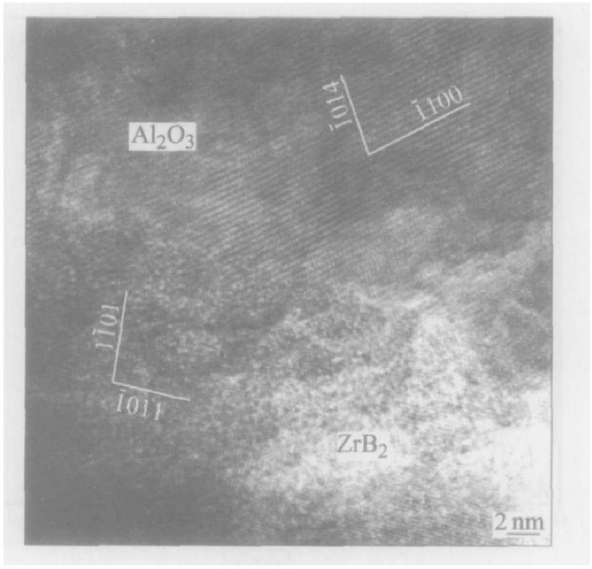

Fig. 6 HREM image of interface of ZrB_2/Al_2O_3 composite powders

reactions happen:

$$3ZrO_2(s) + 4Al(l) \rightarrow 3Zr(s) + 2Al_2O_3(s) \quad (3)$$

$$Zr(s) + 2B(s) \rightarrow ZrB_2(s) \quad (4)$$

From the above analysis, the process of physico-chemical change can be summarized: loss of absorbed water $\rightarrow$ melting of $B_2O_3 \rightarrow B_2O_3(l) + 2Al(s) = 2B(s) + Al_2O_3(s) \rightarrow$ melting of $Al \rightarrow 3ZrO_2(s) + 4Al(l) = 3Zr(s) + 2Al_2O_3(s)$ and $Zr(s) + 2B(s) = ZrB_2(s)$. An amount of Al_2O_3 particles form prior to the ZrB_2 particles during the synthesis procedure. As Ref. [16] has pointed out, there are a large number of defects on the edge of the sub-micron Al_2O_3 particles and the edges of particles show the characteristic of a stepped structure. This morphology is beneficial to nucleation and growth by reducing the nucleation work of compound process. Such microstructure of Al_2O_3 particles creates the energy condition for the nucleation of the ZrB_2 crystals formed later. It can be concluded that ZrB_2 tends to crystallize and grow on the Al_2O_3 particles surface with surface defects acting as nucleation centers. This crystallization process results in good bonding interface between ZrB_2 and Al_2O_3 particles.

From the microstructure, in composite powders, ZrB_2 and Al_2O_3 particles bond well. The good interface makes ZrB_2 particles separated each other by Al_2O_3 particles and can inhibit the grain growth in the particles and finally lead to decrease in the particle size. The small particle size is of advantage to the powder sintering. It can be predicted that the ZrB_2/Al_2O_3 composite powders fabricated by SHS with reductive process will exhibit good formability and sintering performance.

REFERENCES

[1] Mishra S K, Das S, Das S K, et al. Sintering studies on ultrafine ZrB_2 powder produced by a self-propagating high-temperature synthesis process [J]. J Mater Res, 2000, 15: 2499-2506.

[2] Plovnick R H, Richards E A. New combustion synthesis route to TiB_2-Al_2O_3 [J]. Materials Research Bulletin, 2001, 36: 1487-1493.

[3] Upadhga K, Yang J M, Hoffmann W P. Materials for ultrahigh temperature structural applications [J]. Am Ceram Soc Bull, 1997, 58: 51-56.

[4] Mroz C. Annual mineral review—zirconium diboride [J]. Am Ceram Soc Bull, 1995, 74: 158-165.

[5] Low I M. Combustion synthesis of zirconium boride ceramics [J]. Key Engineering Materials, 1991, 53-55: 592-597.

[6] Khanra A K, Pathak L C, Mishra S K. Self-propagation-high-temperature synthesis of ultrafine ZrB_2 powder [J]. J Mater Sci Lett, 2003, 22: 1189-1191.

[7] Radev D D, Marinov M. Properties of titanium and zirconium diborides obtained by self-propagated high-temperature synthesis [J]. Journal of Alloys and Compounds, 1996, 244: 48-51.

[8] Klinger L, Gotman I, Horvitz D. In situ processing of TiB_2/TiC ceramic composites by thermal explosion under pressure: experimental study and modeling [J]. Mater Sci Eng, 2001, A302: 92-99.

[9] ZHANG Ting-an, YANG Huan, NIU Li-ping, et al. Kinetics of preparation of titanium boride by SHS [J]. The Chinese Journal of Nonferrous Metals, 2001, 11(4): 567-570. (in Chinese)

[10] DOU Zhi-he, ZHANG Ting-an, HOU Chuang, et al. Elementary research on CaB_6 prepared by SHS [J]. The Chinese Journal of Nonferrous Metals, 2004, 14(2): 322-326.

[11] Hideaki I, Tsuneaki M, Shigeharu N. Reaction control of TiB_2 formation from titanium metal and amorphous boron [J]. J Mater Sci, 1989, 24: 420-425.

[12] Zhang X H, Xu Q, Han J C. Self-propagating high temperature combustion synthesis of TiB/Ti composites [J]. Mater Sci Eng, 2003, A348: 41-46.

[13] Mu B C, Yu J Y, Li Q. Research on SHS Ti-Al based porous material [J]. The Chinese Journal of Nonferrous Metals, 2002, 12(1): 48-53.

[14] Subrahmanyam J, Rao R M. Combustion synthesis of $MoSi_2$-SiC Composites [J]. J Am Ceram Soc, 1995, 78(2): 487-490.

[15] SU Juan, LI Jun, QIAN Dong-hao. Al_2O_3 matrix porous ceramics prepared by SHS [J]. The Chinese Journal of Nonferrous Metals, 2004, 14(7): 1234-1240.

[16] Yu Z Q, Wu G H, Sun D L. Rare-earth oxide coating for sub-micro particulates reinforced aluminum matrix composite [J]. Mater Sci Eng, 2003, 357A: 61-66.

(Edited by YANG Bing)